Coil Performance and Evaluation of Pavement Durability of Dynamic Wireless Power Transfer System using Ferrite-less and Capacitor-less Coil for Road Construction Methods

Takehiro Imura[1)] Koki Hanawa[1)] Kanta Sasaki[1)] Nagato Abe[2)]

1) Tokyo University of Science, Noda, Chiba, Japan

2) Toa Road Corporation, Roppongi, Tokyo, Japan

ABSTRACT: The development of technology for embedding coils in roads is important for dynamic wireless power transfer (DWPT). When embedding coils in a road, it is necessary to ensure both the electrical and mechanical properties required for DWPT. In this study, coils are produced using PP and PE, which are synthetic resins. In addition, the coil is mainly an open-type coil without the ferrite and capacitor. The electrical characteristics of the coil were evaluated before and after burying it. Further, we evaluated the mechanical strength of the road before and after the coils were buried using the falling weight deflectometer test. Four construction methods were investigated. The deformation of the inside of the coil was measured using strain gauges, and during paving, the effect of the heat of the asphalt in the space inside the coil was measured using thermocouples. A comprehensive evaluation of the electrical and mechanical properties of the synthetic resin coils was conducted when they were paved. The results show that the reflection crack suppression sheet (RC mesh) method is currently the best construction method. Moreover, it was found that injecting cement grout to protect the coil was the best way to reduce the residual strain.

KEY WORDS: Dynamic wireless power transfer, ferrite-less and capacitor-less coils, road pavement, synthetic resin

1. Introduction

Global warming is an unavoidable issue that must be considered by the transportation sector. Dynamic wireless power transfer (DWPT) [(1)-(11)] has attracted significant attention as a sustainable system to reduce CO_2 emissions in the transportation sector. There are two types of DWPTs: magnetic field coupling and electric field coupling. The magnetic field method is used because it is more resistant to rain. The cost of the coils accounts for 1/4 of the total cost of equipment and construction for the installation of the DWPT system, and if the cost can be reduced, the economic viability of DWPT will increase. In this study, ferrite-less and capacitor-less coils[(12)-(14)], which are low-cost coils, are embedded in roads to achieve the requisite electrical and mechanical properties. Four construction methods have been tested. The electrical characteristics, efficiency, and power are verified. As for the mechanical properties, we verified the strength of the coil itself using strain gauges. Furthermore, the effect of heat from the asphalt mixture generated during pavement construction was studied. The structural strength of the road pavement was evaluated by a deflection measurement test using falling weight deflectometer (FWD). Then, after verifying the bearing capacity of cracks on the road, the service life of the road was calculated. Finally, a comprehensive evaluation of the electrical and mechanical properties was conducted.

2. DWPT system configuration

This section describes the overall project and the DWPT system.

2.1. DWPT road and measurement environment

The experiment was conducted by burying the coil in a section of a 110 m DWPT road at the Noda campus of Tokyo University of Science. An aerial view of the test site is shown in Fig.1. In this study, only coil-to-coil evaluations were performed to measure the characteristics accurately, although the environment here allows experiments at speeds of up to 70 km/h. The measurement environments of the transmitting and receiving coils before and after the burial are shown in Fig.2.

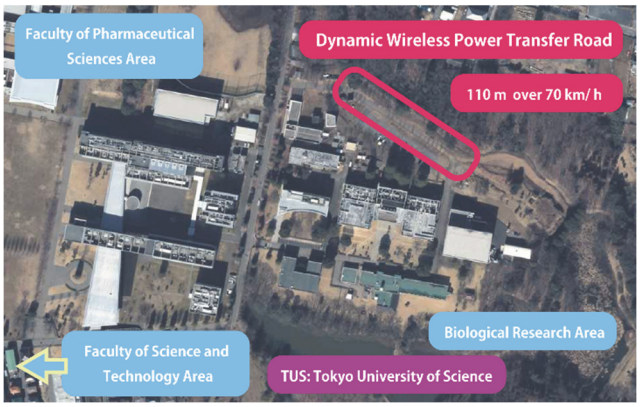

Fig.1 Aerial view of the running feeder section. This figure was created by processing an aerial photograph taken by the Geospatial Information Authority of Japan (taken in 2013).

Fig.2 Transmitting and receiving coils' measurement environments before and after burial

2.2. Four construction methods: Case 1 to Case 4

The four construction methods shown in Fig.3 are described as follows: Case 1: covering the coils with an RC mesh sheet; Case 2: placing unreinforced cement concrete retaining plates under the coils and covering the coils with an reflection crack suppression (RC mesh) sheet; Case 3: wrapping the coil horizontally and vertically with stretch film and winding it vertically and horizontally three times; Case 4: injecting cement grout around the

coil. The transmitting coil sizes and types are listed in Table 1. A list of construction methods is presented in Table 2.

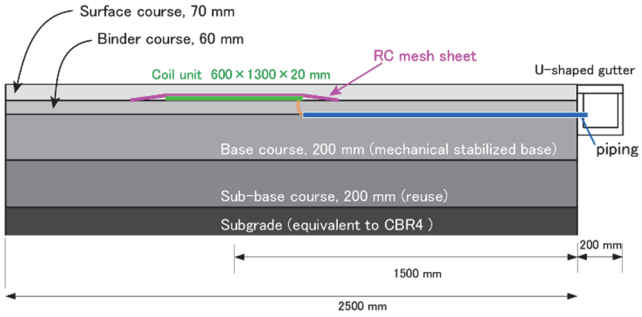

(a) RC mesh sheet

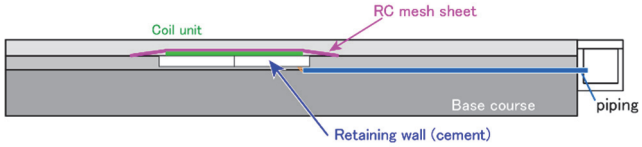

(b) Retaining wall (cement) and RC mesh sheet

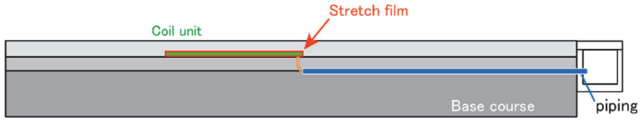

(c) Stretch film

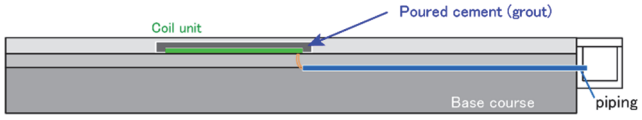

(d) Cement (grout)

Fig.3 Four methods of coil burial

Table 1 Power transmission coil specifications

Coil size (Case size)	600 × 1300 mm (694 × 1380 × 20 mm)
Turns	36
Interlayer gap	1 mm
Line pitch	7 mm
Conductor diameter	3 mm
Weight	PP: 22.5 kg, PE: 23.6 kg

Table 2 List of construction methods

Number of Cases	Construction method	Material
Case1	RC mesh	PP (top and bottom layer)
Case2	Retaining wall & RC mesh	PP (top and bottom layer)
Case3	Stretch film	PP (top and bottom layer)
Case4	Cement (grout)	PE (top and bottom layer)
Common feature	-	PE (middle layer)

The power receiving coil is shown in Fig.4. The parameters used are listed in Table 3. The Q-value of the power receiving coil is over 200, although it has not been optimized.

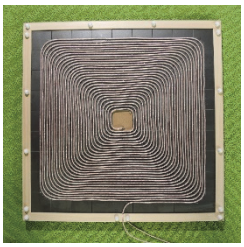

Fig.4 Power receiving coil

Table 3 Power receiving coil specifications

Coil size	400×400 mm
Turns	30
Line pitch	6 mm
Conductor diameter	3 mm
Total length of line	≒30 m
Weight	8.57 kg

3. Coil embedded road construction

The flow of the coil burial work is shown in Fig.5. Cutting and pre-treatment of the pavement is necessary for embedding a coil in an existing road. After laying the base course (mechanically stabilized crushed stone) and installing the piping, binder course work was performed. The coils were then installed and wired, and four construction methods were performed. Finally, the pavement was completed by paving the surface of the asphalt mixture. The details of the four construction methods are shown in Fig.6 to Fig.9.

(a) Cutting (b) Removal of asphalt mixture

(c) Base course (MSCS) (d) Piping setup

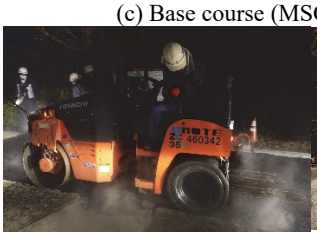

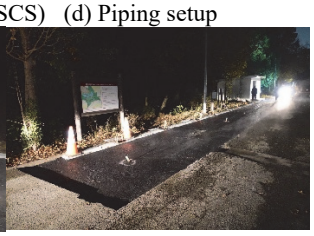

(e) Binder course (f) Finished binder course

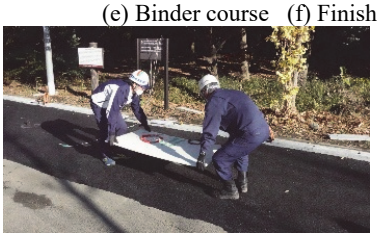

(g) Coil installation 1 (h) Coil installation 2

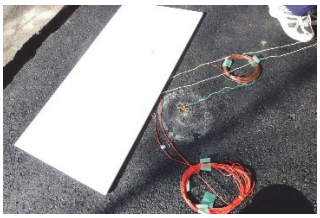


(i) Before wiring (j) Wiring work

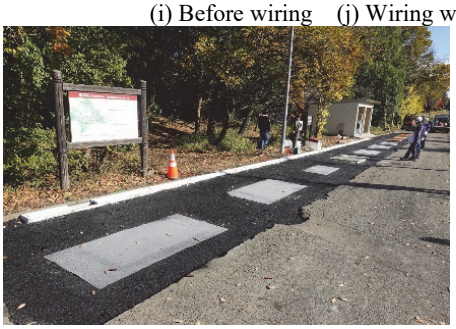


(k) Complete coil installation and wiring using the four methods


(l) Paving of surface course (m) Finished pavement

Fig.5 Flow of coil burial work


(a) Laying of RC mesh (b) Finished RC mesh

Fig.6 Case 1: RC mesh


(a) Soil retaining board (b) Soil-retaining board after burial


(c) Coil installation (d) Completed RC mesh

Fig.7 Case 2: soil retaining board and RC mesh


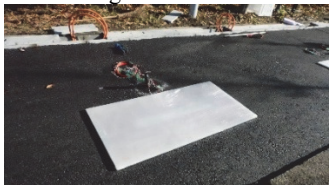

(a) Film winding (b) Completion

Fig.8 Case 3: stretch film


(a) Cement grout into formwork (b) Surface finish

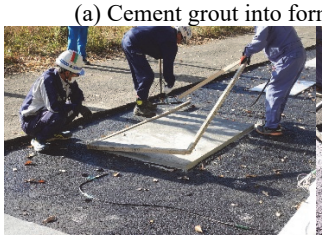


(c) Removal of formwork. (d) Finished

Fig.9 Case 4: Grout material, cement for pouring

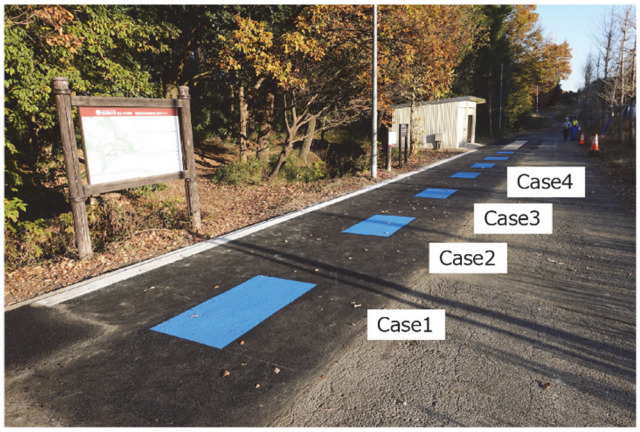

Fig.10 Post-construction painting of the four cases

After the coils were embedded, they were painted, as shown in Fig.10 to show where they were embedded.

4. Electrical characteristics of coils

In this section, we discuss the electrical characteristics of the system. The main coil used in this study is an open-type coil, which is called the ferrite-less and capacitor-less coil. The open-type and short-type coils are shown in Fig.11. The open-type coil uses self-resonance owing to stray capacitance, and thus does not require an external resonant capacitor. Moreover, it does not require ferrite, because it is sufficiently efficient. Therefore, only a litz wire is needed to form the coil, which enables cost reduction compared to conventional short-type coils.

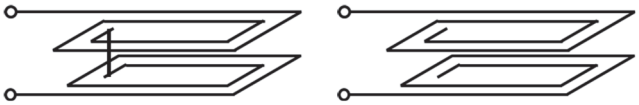

(a) Short type (b) Open-type

Fig.11 Schematic of open and short coils

4.1. Case selection for DWPT buried open coil

This open-type coil is made of litz wire and case only, and it has a three-layer structure with grooves for winding the coil on the upper and lower layers. There is an intermediate layer between the upper and lower layers to secure the separation distance between the upper and lower layers. The middle layer was composed of PE.

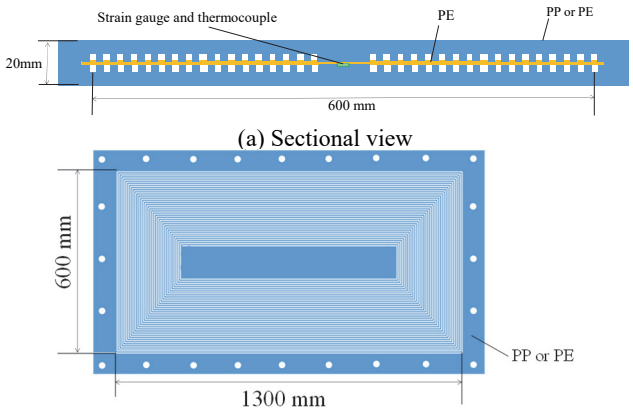

(a) Sectional view

(b) Top view

Fig.12 Coil structure

Open type coils use floating capacitance, so the electric field component near the litz wire is larger than that near the short type. Therefore, it is susceptible to dielectric loss due to tan δ of the coil. A material with low tan δ will have high efficiency and high power. It is also necessary to consider mechanical strength and cost. The characteristics of typical resins are shown in Table 4.

ABS and polycarbonate (PC) are not candidates because they have large tan δ values and are expected to adversely affect efficiency. Extruded polystyrene foam (XPS) is not a candidate because its mechanical strength is very poor.

From the above, we adopt PP and PE because their mechanical strength is not poor, and their efficiency and power are expected to be high. Because the tan δ values of the PP and PE materials were almost the same, PE was also used in this experiment. PP is used in construction methods 1 to 3, and PE is used in construction method 4.

Table 4 Candidate coil case materials

	PE	PP	ABS	XPS	PC
tanδ (1 kHz)	Excellent 0.0005	Good 0.0005~ 0.0018	Fair 0.004~ 0.007	Excellent 0.0001~ 0.0003	Poor 0.021
Bending strength [kg/cm^2]	Poor 7	Good 422~562	Excellent 696~914	Poor 20	Excellent 949~960
Compression strength [kg/cm^2]	Poor 199~253	Good 387~562	Excellent 738~879	Very Poor 16	Excellent 780~879
Deflection temperature under load [°C]	Poor 43~54	Poor 49~60	Good 93~107	Good 80	Excellent 132~137
Insulation strength [kV/mm]	Good 450~500	Excellent 500~660	Fair 350~500	Excellent 500~700	Fair 400
Material cost (1000×2000 ×12 mm)	Poor 54,890 yen	Good 11,495 yen	Fair 43,494 yen	Excellent 1362 yen (910×1820 ×20 mm)	Fair 38,000 yen

A photograph of the coil used is shown in Fig.13. As mentioned earlier, the structure is the same for all the coils and consists of three layers: the top, middle, and bottom layers.

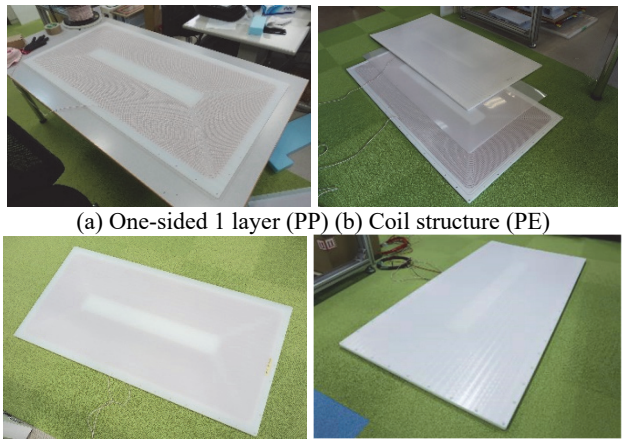

(a) One-sided 1 layer (PP) (b) Coil structure (PE)

(c) Finished form (PP) (d) Completed form (PE).

Fig.13 Photograph of open type coil

4.2. Coil electrical characteristics before and after burial

The locations of the sending and receiving coils and the relationship between the surface course and binder course are shown in Fig.14. The distance between the coils was 140 mm, and the gap between the ground and the receiving coil was 90 mm.

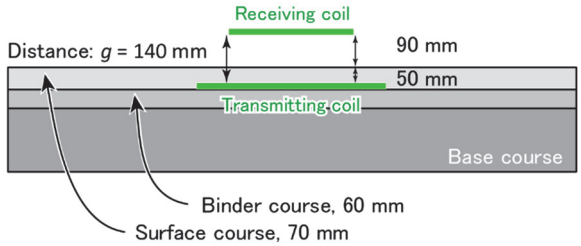

Fig.14 Distance between transmitting and receiving coils and road structure

The parameters of the coils measured in the room before and after embedding the coils in the road are listed in Table 5. In general, the resistance increased and the Q-value decreased after the coil was embedded, and the coil characteristics deteriorated. In particular, the Q-values of cases 2 and 4 using cement deteriorated significantly to less than 100. By contrast, the Q-values of cases 1 and 3 were above 100, although they deteriorated.

Table 5 Coil characteristics before and after burial

Construction Method	Timing	f_0 [kHz]	R [Ω]	Q ($=\omega L/R$)	L [mH]	C [nF]
Case1	Before	76.2	2.71	391	2.21	19.7
	After	64.6	5.27	191	2.49	2.44
Case2	Before	69.8	2.43	411	2.27	2.29
	After	69.8	30.9	25.7	1.81	2.87
Case3	Before	84.8	2.61	438	2.15	1.64
	After	60.8	6.97	132	2.41	2.84
Case4	Before	78.6	2.33	432	2.04	2.23
	After	60.4	14.6	59.1	2.27	3.05

Fig.15 shows the efficiency and power against frequency, and Fig.16 shows the efficiency and power against the load. Table 6 and Table 7 show the efficiency and power before and after the coils were buried in the road, and Table 8 shows the power before and after the coils were buried in the road at 85% efficiency. The resonant frequency deviates from 85 kHz because the stray capacitance deviates from the design before the coil is embedded. As for the effect of coil embedment under the road, it can be said

that the frequency changes significantly when dealing with cementitious materials in cases 2 and 4. In addition, the burial of the coil under the road reduces efficiency and power. The maximum efficiency was over 98% in Case 1, but the power was less than 3 kW, and the efficiency was over 91% in Case 3. Cases 2 and 4 are construction methods using cement-based materials, and their efficiency is less than 80%. Considering the case where the efficiency is more than 85%, the power was more than 14 kW before the coils were buried, but after the coils were buried, the power was 4.8 kW for Case 1. The power values were converted to 600 V input.

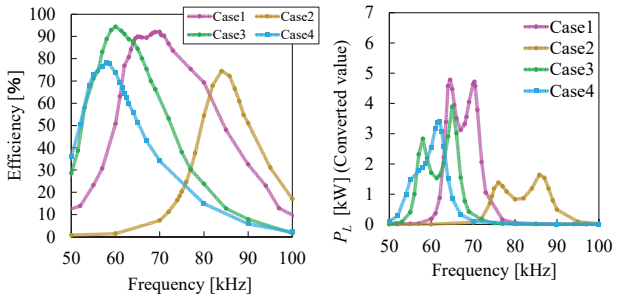

Fig.15 Efficiency and power against frequency after the coils are buried

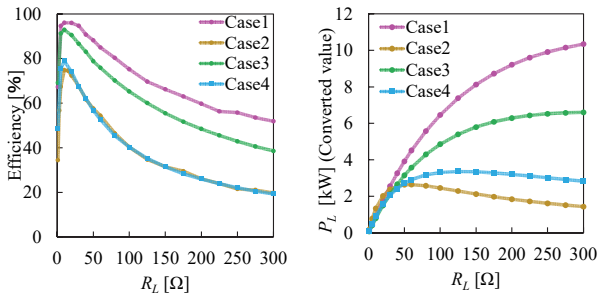

Fig.16 Efficiency and power against load after the coils are buried

Table 6 Efficiency and power before coils are buried

	Case1	Case2	Case3	Case4
Frequency [kHz]	68.8	67.5	64.0	72.3
R_{Lopt}	18	18	16	21
η_{max} [%]	97.1	97.1	96.6	97.1
$P_{L,\ \eta max}$[kW] (Converted value)	2.3	2.3	2.3	2.5

Table 7 Efficiency and power after burial

	Case1	Case2	Case3	Case4
Frequency [kHz]	68.4	85.8	61.3	58.6
R_{Lopt}	10	15	10	10
η_{max} [%]	96.0	73.6	92.8	78.9
$P_{L,\ \eta max}$[kW] (Converted value)	2.7	1.4	1.4	1.4

Table 8 Power before and after burial (converted value)

Construction method	Timing	>85%
Case1	Before	14.1 kW
	After	4.8 kW
Case2	Before	14.5 kW
	After	-
Case3	Before	15.5 kW
	After	3.4 kW
Case4	Before	15.7 kW
	After	-

5. Mechanical properties of coils

The mechanical properties of the coils were evaluated to check the effect of distortion caused by rolling during road paving and the effect of heat from asphalt exceeding 100 °C during paving. Fig.17 shows a photograph of the strain gauges and thermocouples installed in the center of the coil in the first layer. The position of the thermocouple on the roadside is shown in Fig.18.

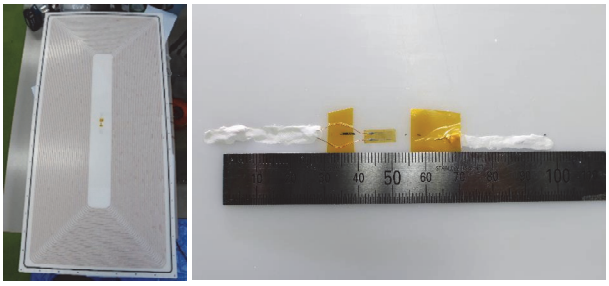

(a) Overview (b) Strain gauge (left) and thermocouple (right)

Fig.17 Position of strain gauge and thermocouple in the coil

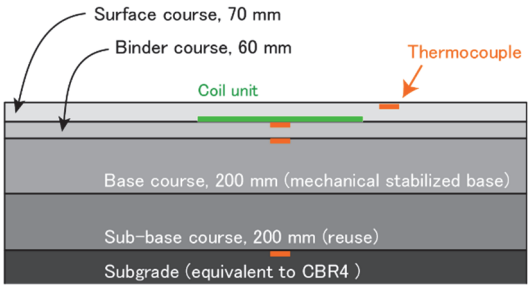

Fig.18 Position of thermocouple in the road

The internal temperature of the pavement while adding asphalt is shown in Fig.19. The surface and base course were above 100 °C, while the asphalt surface was above 145 °C. The base course and subgrade were not significantly affected by the heat. Fig.20 shows the temperature of the coil. The temperature of the coil is affected by the load deflection temperature and needs to be improved.

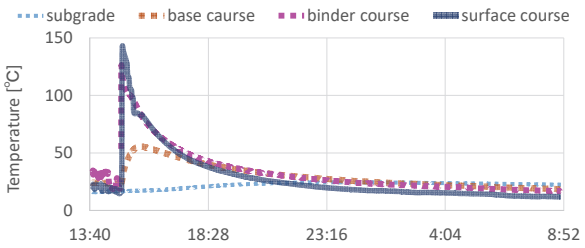

Fig.19 Internal temperature of the pavement

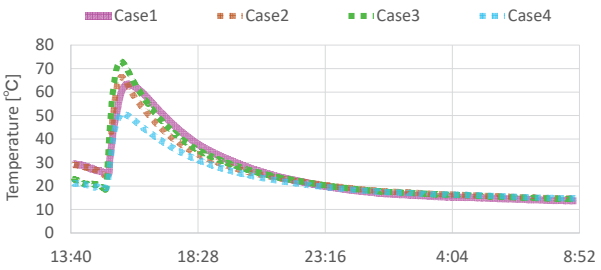

Fig.20 Temperature at the center of the coil unit

Fig.21 shows the strain of the coils. During the paving work, the distortion is as expected because of the rolling pressure from the roller, but after the laying work, residual strains were observed.

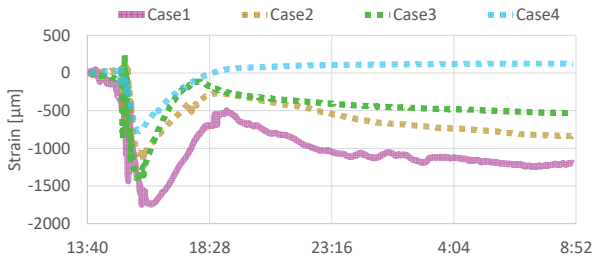

Fig.21 Strain at the center of the coil unit

In Case 1, the residual strain was large; in Case 3, the center temperature of the stretch film was the highest at 73.1 °C, whereas in Case 4, the cement pouring method using grout material showed the lowest residual strain. The maximum center temperature was 50.8 °C, which was lower than the others.

6. Mechanical characteristics of road pavement

Regarding the mechanical properties of the road, the amount of deflection from the FWD test and the number of years the road can be used, calculated from the FWD test, will be verified.

6.1. Impact on roads

The FWD test was used to evaluate the bearing capacity with respect to the cracks. The FWD test scene is shown in Fig.22. The results of the deflection measurement of the road pavement by FWD are shown in Fig.23. The deflection in cases 1 and 3 is 1.1 mm. The deflection of a typical pavement without coils is 0.8 mm.

The deflection of Case 2 with unreinforced concrete soil-retaining plates was 1.85 mm, and that in Case 4 where coils were covered with cement grout was 1.36 mm, which is larger than that of the general section without coils. It is presumed that the lack of adhesion between the asphalt mixture and cementitious material caused a larger strain inside the coil.


(a) Positioning (b) FWD test vehicle and sensors

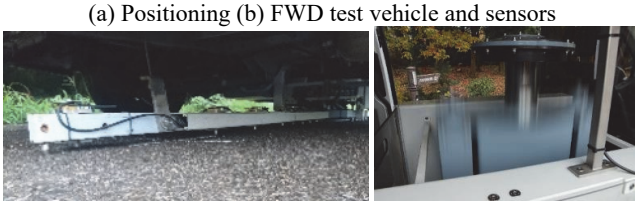
(c) Deflection sensor (d) Falling weight

Fig.22 Deflection measurement test by falling weight deflectometer (FWD) test

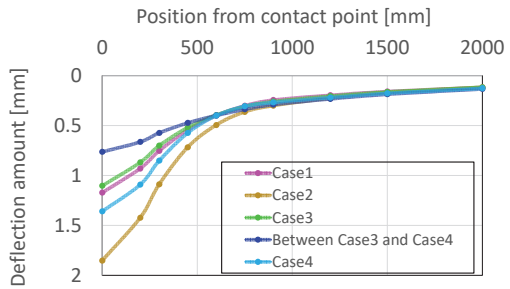

Fig.23 Deflection of road pavement

6.2. Allowable driving years

The allowable driving years calculated from the FWD test are listed in Table 9. The N5 traffic volume is assumed to be 250–1000 heavy vehicle traffic per day, and the N6 traffic volume is assumed to be 1000–3000 heavy vehicle traffic per day. A total of 255 vehicles for N5 and 1275 vehicles for N6 were used as representative values in the calculation.

In cases 1 and 3, the number of fatigue fracture wheels is more than 70,000 cycles with a design wheel load of 49 kN, and more than 3.4 million cycles with a design wheel load of 17 kN for small roads. The general section without coils can tolerate more than 365,000 cycles at a design wheel load of 49 kN, and the value with coils is approximately five times that without coils.

If the operation is between wheels with a few wheels passing positions, the probability of a wheel passing over the coil is 2.4% [15]. Considering this, the allowable driving years is expected to be 16 to 34 years for the N5 traffic equivalent road. It is also judged that the system can be in service for more than six years for N6 traffic volume equivalent road.

Table 9 Number of years the road can be traveled

	Case1	Case2	Case3	Case4
Limitation on the number of loaded wheels (17kN)	3,423,500	698,600	3,925,500	1,668,100
Number of trip limits (17kN)	140,026,472	28,573,826	160,559,052	68,227,883
Limitation on the number of loaded wheels (49kN)	77,800	36,900	71,200	46,100
Number of trip limits (49kN)	3,182,141	1,509,267	2,912,191	1,885,562
Road life [years] (N5)	34.2	16.2	31.3	20.3
Road life [years] (N6)	6.8	3.2	6.3	4.1

From Table 9, the overall evaluation of the electrical and mechanical properties of the coil and the mechanical properties of the road shows that Case 1, Case 3, Case 4, and Case 2 are superior, in that order. However, even in Case 1, there is still room for improvement because the problem of residual strain has not been solved and the coil cannot be used for 10 years at the equivalent of N6 traffic volume.

Table 10 presents the overall evaluation of the five stages. The overall evaluation is unfavorable for cases 2 and 4 because of their low efficiency. However, Case 4 was promising because of its ability to reduce residual strain. Case 3 is the cheapest in terms of cost but has no outstanding features. Although Case 1 has some issues with residual strain, it has the highest overall rating because of its high efficiency, large albeit insufficient power, and high road pavement durability.

Table 10 Construction method 5-step comprehensive evaluation

Category	Evaluation	Case1: RC mesh	Case2: Retaining wall & RC mesh	Case3: Stretch film	Case4: Poured cement (grout)
Electrical characteristics, coil	Efficiency	5	2	4	2
	Power	3	1	1	1
Mechanical properties, coil	Temperature	4	4	3	5
	Residual strain	2	3	3	5
Mechanical properties, road	Durability (FWD)	3	1	3	2
Other	Workability	5	3	3	4
Total	Overall evaluation	5	1	4	2

7. Conclusion

In this study, coils were produced using synthetic resins, PP and PE. The coils were mainly open-type coils without ferrite or capacitors. The electrical and mechanical properties of the coils were evaluated before and after burying them. Next, the mechanical strength of the road before and after the burial of the coils was evaluated using the FWD test. Four construction methods were investigated. Strain gauges were used to measure the deformation inside the coils, and thermocouples were used to measure and evaluate the effect of the heat of the asphalt mixture on the space inside the coils during paving. The efficiencies of cases 2 and 4 were low owing to the pronounced influence of cementitious materials. Considering the efficiency, power, and road durability, Case 1 with the RC mesh had the highest overall evaluation. Future work could include the design of coils for higher power, investigation of the cause of the decrease in efficiency after burial, residual strain, and increasing the bearing capacity of the road pavement.

ACKNOWLEDGMENT

This research was partly carried out as “A study on coil burial for dynamic wireless power transfer,” by the commissioned research of National Institute for Land and Infrastructure Management under technology research and development system of the Committee on Advanced Road Technology established by MLIT, Japan, and partly supported by JSPS KAKENHI Grant Number 17H04915.

REFERENCES

(1) G. A. Covic and J. T. Boys, "Modern Trends in Inductive Power Transfer for Transportation Applications," IEEE Journal of Emerging and Selected Topics in Power Electronics, vol. 1, no. 1, 2013, pp. 28-41.

(2) Su Y. Choi, Beom W. Gu, Seog Y. Jeong, Chun T. Rim, "Advances in wireless power transfer systems for roadway-powered electric vehicles," IEEE Journal of emerging and selected topics in power electronics, Vol.3, No.1, 2014, pp.18-36.

(3) K. Song, C. Zhu, K. E. Koh, D. Kobayashi, T. Imura, and Y. Hori, "Modeling and design of dynamic wireless power transfer system for EV applications," IECON 2015-41st Annual Conference of the IEEE Industrial Electronics Society, 2015 , pp.005229-005234.

(4) D. Kobayashi, K. Hata, T. Imura, H. Fujimoto, and Y. Hori, “Sensorless Vehicle Detection Using Voltage Pulses in Dynamic Wireless Power Transfer System,” The 29th International Electric Vehicle Symposium and Exhibition, 2016

(5) C. C. Mi, G. Buja, S. Y. Choi, and C. T. Rim, “Modern advances in wireless power transfer systems for roadway powered electric vehicles,” IEEE Transactions on Industrial Electronics, vol. 63, no. 10, pp. 6533–6545, 2016.

(6) K. Hata, K. Hanajiri, T. Imura, H. Fujimoto, Y. Hori, M. Sato, and D. Gunji, "Driving Test Evaluation of Sensorless Vehicle Detection Method for In-motion Wireless Power Transfer," 2018 International Power Electronics Conference (IPEC-Niigata 2018-ECCE Asia), 2018, pp.663-668.

(7) C. Wang, P. Wang, Q. Zhu, and M. Su, "An Alternate Arrangement of Active and Repeater Coils for Quasi-Constant Power Wireless EV Charging," 2019 IEEE PELS Workshop on Emerging Technologies: Wireless Power Transfer (WoW), 2019.

(8) M. Maemura and A. Wendt, "Dynamic Power Transfer as a Feature - Employing Stationary WPT Devices for Dynamic Operation," pp. 50-55, 2020.

(9) V. Z. Barsari, D. J. Thrimawithana, G. A. Covic, and S. Kim, "A Switchable Inductively Coupled Connector for IPT Roadway Applications," vol. 1, no. Icc, pp. 35-39, 2020.

(10) B. J. Varghese, A. Kamineni, N. Roberts, M. Halling, D. J. Thrimawithana, and R. A. Zane, "Design Considerations for 50 kW Dynamic Wireless Charging with Concrete-Embedded Coils," pp. 40-44, 2020.

(11) R. M. Nimri, A. Kamineni, and R. Zane, "A Modular Pad Design compatible with SAE J2954 for Dynamic Inductive Power Transfer," pp. 45-49, 2020.

(12) Koichi Furusato, Takehiro Imura and Yoichi Hori, "Improvement of 85 kHz Self-resonant Open End Coil for Capacitor-less Wireless Power Transfer System," 2016 Asian Wireless Power Transfer Workshop, Dec. 2016.

(13) Yoshiaki Takahashi, Takehiro Imura and Yoichi Hori, "Comparison of 85 kHz Self-resonant Open-end Coils with Different Types of Wire for Capacitor-less Wireless Power Transfer System," 2017 Asian Wireless Power Transfer Workshop, Dec. 2017.

(14) Yoshiaki Takahashi, Katsuhiro Hata, Takehiro Imura and Yoichi Hori, "Comparison of Capacitor- and Ferrite-less 85kHz Self-resonant Coils Considering Dielectric Loss for In-motion Wirelss Power Transfer," The 44th Annual Conference of the IEEE Industrial Electronics Society, Oct. 2018.

(15) Saburo Matsuno, Taisuke Kobayashi, “About the Vehicle Driving Position”, The 14th Japan Road Conference, pp. 177-178, 1981 (in Japanese)